Development of an Early Prediction Model for Subarachnoid Hemorrhage With Genetic and Signaling Pathway Analysis

Development of an Early Prediction Model for Subarachnoid Hemorrhage with Genetic and Signaling Pathway Analysis

Wanjing Lei [1], Han Zeng [2], Hua Feng [3], Xufang Ru[3], Qiang Li[3], Ming Xiao[1], Huiru Zheng[4], Yujie Chen[3]* and Le Zhang[1,2]*

[1] College of Computer Science, Sichuan University, Chengdu, 610065, China

[2]College of Computer and Information Science, Southwest University, Chongqing, 400715, China

[3]Department of Neurosurgery, Southwest Hospital, Third Military Medical University, Chongqing, 40038, China

[4]School of Computing, Ulster University, N. Ireland, BT37 0QB, UK

*** Correspondence:**
Prof. Le Zhang
zhangle06@scu.edu.cn

Prof. Yujie Chen
yujiechen6886@foxmail.com

Keywords: Bioinformatics[1], Genomics[2], Big Data[3], Artificial Intelligence[4], Genetics[5].

Abstract

Subarachnoid hemorrhage (SAH) is a devastating disease with high rates of mortality and disability and a poor clinical prognosis. It has been the focus of much attention in both basic and clinical medical research. Here, we investigate therapeutic drugs and effective targets for early prediction of SAH. First, we demonstrate that LCN2 can be used to effectively intervene in or treat SAH from a cell signaling pathway perspective. Next, three potential genes that we explored are validated by manual review of experimental evidence. Finally, we demonstrate that the ensemble learning model for early SAH prediction performs better than the classical logistic regression, support vector machine, and naive-Bayes models.

1 Introduction

Subarachnoid hemorrhage (SAH) is the fastest developing and most critical hemorrhagic cerebrovascular disease, accounting for 5% of cerebrovascular diseases (Macdonald, 2014), and is associated with high rates of mortality and disability and poor clinical prognosis (Suarez et al., 2006). Although there have been significant advances in diagnostic methods, surgery, and endovascular techniques in recent years, the mortality rate of SAH remains as high as 15% (Macdonald et al., 2008).

The total length of the article is about 3300, including 4 figures in total.

Recent research has shown that early brain injury (EBI) may be the main cause of poor prognosis in SAH patients. Therefore, current SAH studies focus on exploring therapeutic drugs and targets for reduction of EBI after SAH and the early prediction of SAH (Sozen et al., 2011).

Lipocalin 2 (LCN2) is an acute secretory protein that regulates the pathophysiological processes of various organ systems in mammals and participates in the intrinsic immune protection of the central nervous system (CNS) (Flo et al., 2004;Ferreira et al., 2015). Studies of acute white matter injury in a mouse SAH model and the role of LCN2 in injury (Egashira et al., 2014) indicate that LCN2 plays an important part in SAH-induced white matter injury. Since above evidences suggest that LCN2 is closely related to SAH, we propose our first research question: is specific intervention for LCN2 (Warszawska et al., 2013) a promising SAH treatment strategy?

On the other hand, most previous studies (Chu et al., 2011;Ni et al., 2011;Zhang et al., 2017a) have only explored biomarkers for SAH prediction and treatment in a narrow molecular range, rather than taking a genome-wide approach. We propose our second research question: could we use a genome-wide approach to find potential biomarkers for SAH based on the effects of LCN2 treatment?

Previous studies have usually predicted SAH based on diagnostic imaging (Frontera et al., 2006;Ramos et al., 2019) and clinical automation data (Roederer et al., 2014), which may not provide enough predictive power. Thus, we propose our third research question: could we use key genes to build a more powerful early prediction model for SAH?

In this paper, we propose a new research plan to answer the above three research questions. First, we use SAH intervention experiments to screen out candidate genes that are susceptible to LCN2, then employ Fisher's exact test (Xie et al., 2011;Li et al., 2017;Xia et al., 2017;Zhang et al., 2019b) to choose signaling pathways from among the candidates under different experimental conditions. Second, we use e-Bayes (Carlin and Louis, 2010), SVM-RFE (Duan et al., 2005), SPCA (Zou et al., 2006), and statistical tests (Zhang et al., 2016;Zhang et al., 2018;Xiao et al., 2019b;Zhang et al., 2019b;Zhang et al., 2019d;Zhang et al., 2020) to investigate key genes from experimental data by considering both SAH and LCN2 as factors. Third, we integrate the logistic regression (LR), support vector machine (SVM), and naive-Bayes algorithms (Xia et al., 2017;Zhang et al., 2017a;Zhang et al., 2019a) into an ensemble learning model (Gao et al., 2017;Zhang et al., 2019b) to build a model for early SAH prediction.

First, manual review of the experimental evidence (Osuka et al., 2006;Majdalawieh et al., 2007;Hanafy et al., 2010;Hao et al., 2014;Kwon et al., 2015;Yu et al., 2018) demonstrates that we could intervene or treat SAH by targeting LCN2 from a cell signaling pathway perspective. Next, we explore three key genes that are sensitive to both SAH and LCN2 treatment, again using manual review of the experimental evidence (Huang et al., 2016;Sabo et al., 2017;Yu et al., 2018) to cross-validate the relationships between SAH and these key genes. Finally, we show that our SAH early prediction ensemble-learning model outperforms the classical LR, naive-Bayes, and SVM models. In summary, we consider that this work provides a novel strategy for the future study of clinical treatment of SAH and related diseases.

2 Materials and Methods

2.1 Experimental configuration

All experimental procedures were approved by the Ethics Committee of Southwest Hospital and were performed in accordance with the guidelines of the National Institutes of Health Guide for the Care and Use of Laboratory Animals.

2.1.1 Intervention experiment for SAH

The original chip data for this experiment were provided by the Department of Neurosurgery, Southwest Hospital, PLA Military Medical University. SAH and sham-operated models were established; details are given in the Supplementary Material. Each experimental group included five mice, and the white matter area of the cerebral cortex was taken for gene chip testing. A total of 10 original chip samples were obtained from the SAH intervention experiments; these were divided equally into two groups as follows.

(1) SAH disease group: brain tissue in the white matter region of the cerebral cortex of SAH mice.

(2) Control group normal-1: brain tissue in the white matter region of the cerebral cortex of normal mice.

The chip was an Affymetrix GeneChip Mouse Gene 1.0 ST Array. Raw data included sample RNA extraction (white matter brain cells from the SAH model and from normal mice), sample RNA quality detection (total RNA>1 ug), cDNA synthesis, sense strand cDNA fragmentation, biotin labeling, chip hybridization, chip elution, and chip scanning. The raw data are available at http://www.ebi.ac.uk/arrayexpress/experiments/E-MTAB-8407.

We then carried out mass analysis and used the R Bioconductor package to perform quality control for each original chip (the SAH disease group and the control group normal-1). In the output gray scale image (Figure S1) for each chip sample, each chip name and the four corner patterns were very clear, and the contrast between light and dark was moderate.

The right panel of Figure 1A shows the Relative Log Expression (RLE) boxplot for these 10 chips. The center of each sample was close to the position RLE=0. This indicates that the expression levels of most genes in the sample were consistent. In addition, Figure S2 describes a normalized unscaled standard errors (NUSE) detection(Marta and Marc, 2014). Since Figure S2 shows that the center of each sample is close to the position NUSE=1, we consider that the samples are too stable to have obvious batch effect. Then, we used Robust Multi-chip Analysis (RMA) (Irizarry et al., 2003) for data preprocessing, including background and perfect match probes (PM) correction, normalization, and summarization, to obtain the probe expression data matrix (Table S1). Finally, clustering analysis(Liu et al., 2019;Xiao et al., 2019a;ZHANG et al., 2019c;Wu and Zhang, 2020) (Figure S3) shows that the major differences between the chip of each group comes from SAH.

2.1.2 Intervention experiment for LCN2

Here, in order to interfere with the expression of LCN2, 2 μL of specific short interfering RNAs (siRNAs) was delivered into the lateral ventricle with a Hamilton syringe. The injection was performed 48 h before SAH and three groups were used, as described below. We detail the procedures in the Supplementary Material.

(1) SAH-siRNA-LCN2: the SAH model was established and treated with intrathecal injection of LCN2 siRNA, and two samples were taken on the first and third days after surgery.

(2) SAH-siRNA-NC: the SAH model was established and treated with intrathecal NC siRNA, and two samples were taken on the first and third days after surgery, which helped us to remove the interference factors associated with the siRNA vector.

(3) Control group normal-2: the brain tissue of the white matter region of the cerebral cortex without any treatment.

The total number of samples in all experiments was 25 (Table 1). RNA sequencing was performed on the samples and the raw data are available at https://www.ncbi.nlm.nih.gov/sra/PRJNA575372.

Table 1

2.2 Workflow of the study

Figure 1

The workflow of the study is illustrated in Figure 1. First, we designed the intervention experiment for SAH detailed in section 2.1.1, which allowed us to obtain the differential genes under different experimental conditions. Based on these differential genes, we could identify the key signaling pathways.

As targeting LCN2 could result in changes in these related signaling pathways (causing remission or promotion of SAH), we consider that LCN2 plays an important part in the entire biological cell process for SAH.

Next, we used an intervention experiment for LCN2 to obtain gene expression levels for diseased and normal mouse brain cells at different time points. Then, we employed commonly used dimensional reduction algorithms to explore three key genes under the impact of both SAH and LCN2 treatment.

Finally, we used these three key genes as classifiers to develop an ensemble learning model for early SAH prediction, the predictive power of which was much better than that of the classic LR, naive-Bayes, and SVM models.

3 Results

3.1 Signaling pathway analysis

3.1.1 Differentially expressed gene selection

We used e-Bayes, one of the most commonly used methods for differential expression analysis (Edwards et al., 2005), to screen the differential genes by setting Fold change ≥ 1.5 and p-value < 0.05. Table S2 lists 2942 differentially expressed genes, accounting for 10.16% of the total number of genes (28,944). Among them, there were 1016 and 1926 genes with upregulated and downregulated expression (Figure S4), respectively.

3.1.2 Pathway analysis

We used Eq. 1 and the data in Table S3 to explore related signaling pathways by carrying out Fisher's exact test (Xia et al., 2017) using Kobas 3.0 (Wu et al., 2006;Xie et al., 2011;Ai et al., 2018) for the differentially expressed genes from Table S2.

$$p_F(n_f, n, N_f, N) = 2 * \sum_{x=1}^{n_f} \frac{\binom{n}{x}\binom{N-n}{N_f-x}}{\binom{N}{N_f}} \quad (1)$$

Here, N is the number of genes in the sample and n is the number of genes contained in the pathway. N_f is the number of differentially expressed genes and n_f is the number of differentially expressed genes included in the pathway.

The Fisher's exact test assumes $H_0: p_1 = p_2$; the alternative hypothesis is $H_1: p_1 \neq p_2$. $p_1$is the probability that the differentially expressed gene will fall in the pathway, and p_2 is the probability that the non-differentiated gene does not fall in the pathway. The p-value (p_F) of Fisher's exact test was obtained by Eq. 1.

Table S2 lists 70 signaling pathways for which the p-value was less than 0.001. LCN2 is a protein involved in MAPK signaling pathways that protects the CNS as part of the innate immune system (Warszawska et al., 2013). Previous studies have shown that LCN2 activates phosphorylation of p38 MAPK, which phosphorylates the Ser168 and Ser170 sites of NFATc4 and inhibits nuclear translocation of NFATc4 (Olabisi et al., 2008). NFATc4 is a key factor in remyelination and closely related to SAH, indicating that white matter damage after SAH is associated with remyelination (Kao et al., 2009;Guo et al., 2017).

Therefore, we hypothesize that LCN2 could promote the phosphorylation of transcription factor NFATc4 and inhibit its nuclear transcription by activating p38 MAPK, thereby preventing remyelination and causing white matter damage after SAH.

3.1.3 LCN2 intervention experimental results analysis

To prove our hypothesis, we designed a LCN2 intervention experiment (Figure 1B) to test whether LCN2 could affect SAH from the perspective of the differential expressed genes and the related signaling pathways.

First, we used the DESeq2 (Varet et al., 2016) method to select differentially expressed genes from SAH-siRNA-LCN2 and normal-2, SAH-siRNA-NC and normal-2, and SAH-siRNA-LCN2 and SAH-siRNA-NC groups on days 1 and 3, respectively(Table 1). The results are shown in Table 2, Table S4, and Figure S5.

Table 2

Next, we used Kobas 3.0 (Wu et al., 2006;Xie et al., 2011;Ai et al., 2018) to carry out Fisher's exact test for the differential genes in Table 2, to identify related signaling pathways (Table S5). Next, we used the manually reviewed evidence (Osuka et al., 2006;Majdalawieh et al., 2007;Hanafy et al., 2010;Hao et al., 2014;Kwon et al., 2015;Yu et al., 2018) to cross-validate the SAH-related signaling pathways in Table S5. Table 3 lists the cross-validated SAH-related signaling pathways.

Table 3

As shown in Table 3, all the experimental groups had SAH-related signaling pathways except the transcriptional misregulation in cancer signaling pathway (Lee and Young, 2013) in the SAH-siRNA-LCN2 (3 day) vs SAH-siRNA-NC (3 day) experimental group. However, as one of the proteins from this pathway, Gzmb (Table S5), is closely associated with post-ischemic brain cell death (Chaitanya et al., 2010), we consider that it could be a new target for secondary brain injury inhibition (Armstrong et al., 2017). Therefore, we conclude that specific intervention for LCN2 is a promising SAH treatment strategy.

3.2 Feature selection

After demonstrating the impact of LCN2 on SAH, we chose potential biomarkers for SAH using a genome-wide approach. Figure 1C shows the workflow used to choose key genes that were not only related to both SAH and LCN2 but were also insensitive to treatment at different time points. Figure 1C shows the following three modules.

(1) SAH intervention experiment module

Owing to the large number of differential genes (Table S2), it was necessary to further narrow down the scope of the screening. First, we used the e-Bayes method (Edwards et al., 2005) to filter the probe expression data matrix (Table S1) by the e-Bayes function of R's limma package (Smyth, 2005). The differential probes were obtained by setting the filter parameters to Fold change ≥ 2 and p-value < 0.05.

Second, we used SVM-RFE (Duan et al., 2005) (Eq. 2) to rank the genes in the probe expression data matrix, and then carried out the t-test and F-test (Zhang et al., 2017b) for the top 100 genes.

$$\begin{cases} \boldsymbol{DJ(i) = (1/2)\alpha^T H\alpha - (1/2)\alpha^T H(-i)\alpha} \\ \boldsymbol{H = y_i y_j K(x_i, x_j)} \end{cases} \quad \textbf{(2)}$$

where y_i and y_j represent the classification labels of probes x_i and x_j, respectively; $K(x_i, x_j)$ is the kernel function, $i, j = 1,2,\ldots,n$; α is obtained by training the SVM classifier; $DJ(i)$ is the sort function; and H is the matrix.

We then combined the results of these two methods to obtain the significant probes for both the e-Bayes and SVM-RFE methods.

Finally, we used the transcription cluster annotation file (version: MoGene-1_0-st-v1) downloaded from the Affy (Gautier et al., 2004) website to extract the gene ID for these probes, resulting in 47 key genes (Table S6).

(2) LCN2 intervention experiment module

We performed t-tests and F-tests (Zhang et al., 2017b) for the key genes (Table S6) in the SAH-siRNA-LCN2 (1 day) vs normal-2 and SAH siRNA-LCN2 (3 day) vs normal-2 groups (Table S4).

There were 15 and 13 statistically significantly differential genes for the SAH-siRNA-LCN2 (1 day) vs normal-2 group (Table S7) and the SAH-siRNA-LCN2 (3 day) vs normal-2 group (Table S8), respectively. Taking the intersection of the results from these two experimental groups gave nine key

genes, Tk1, Cyr61, Nupr1, Dcn, Lum, Olig1, Pcolce2, Slc6a9, and Kcnt2, which were sensitive to both SAH and LCN2 intervention, regardless of treatment, at different time points.

(3) Dimensional reduction module

Next, we employed the SPCA algorithm (Zou et al., 2006;Li et al., 2017) to perform dimensional reduction for the nine key genes. This resulted in five candidate genes (Tk1, Cyr61, Olig1, Slc6a9, and Pcolce2). However, manual review of the experimental evidence indicated that only Cyr61 (Yu et al., 2018), Olig1 (Sabo et al., 2017), and Slc6a9 (Huang et al., 2016) were closely related to SAH, cerebral hemorrhage, and brain injury. Therefore, we considered these three genes (Figure 2, Table S9) to be potential biomarkers for SAH.

Figure 2

3.3 Ensemble learning model

3.3.1 Early SAH prediction model

This study used three classification algorithms, LR (Hosmer Jr et al., 2013), SVM (Suykens and Vandewalle, 1999), and naive-Bayes (Wang et al., 2007) to develop the SAH prediction model, using the selected key genes as the respective classifiers. These three classic methods were then integrated into a novel ensemble learning model to improve the predictive accuracy.

Figure 3 shows the workflow of the SAH prediction model, based on our previous studies (Li et al., 2017;Xia et al., 2017;Zhang et al., 2019b). The key equations of the model are as follows.

$$\boldsymbol{D_t(i) = \frac{1}{n}} \tag{3}$$

$$\boldsymbol{\varepsilon_t = \frac{number\ of\ incorrectly\ classified\ samples}{total\ number\ of\ samples}} \tag{4}$$

$$\boldsymbol{\alpha_t = \frac{1}{2} ln \frac{1-\varepsilon_t}{\varepsilon_t}} \tag{5}$$

$$\boldsymbol{D_{t+1}(i) = \frac{D_t(i)}{sum(D)} \begin{cases} exp(-\alpha_t), if\ h_t(x_i) = y_i \\ exp(\alpha_t), if\ h_t(x_i) \neq y_i \end{cases}} \tag{6}$$

$$\boldsymbol{H_m(x) = sign \sum_{t=0}^{T} \alpha_t h_t(x)} \tag{7}$$

$$\boldsymbol{E_{H_m,} = \sum_{m=1}^{3} P_{H_m}} \tag{8}$$

$$Y(x) = \begin{cases} 1 & E_{H_m} \geq 0.5 \\ 0 & E_{H_m} < 0.5 \end{cases} \quad (9)$$

Here, $D_t(i)$ is the weight distribution, t is the iteration time, i is the index of the sample, and n is the number of the sample. ε_t and α_t are the error rate and weight of each weak classifier h_t, respectively. For a sample set $S = \{(x_1, y_1), (x_2, y_2), \ldots, (x_n, y_n)\}$, x_n are the samples and $y_n \in \{0,1\}$ are the labels; y_i=0 indicates that x_i is not an SAH patient, and y_i=1 indicates that x_i is an SAH patient. H_m is the homomorphic integration for each weak classifier h_t; m is the index of the weak classifier, m=1,2,3; T is the threshold of the iteration time; P_{H_m} is the predictive probability of disease; and $E_{H_m}$is the estimated probability of the model H_m. $Y(x)$ is the result of the final classifier obtained by a voting method (Dietterich, 2000).

Figure 3

3.3.2 Predictive performance comparison

Figure 4A compares the classification performance for the LR, naive-Bayes, SVM, and ensemble learning models, based on four commonly used classification measurements (Table S10) (Zhang et al., 2019b). The numerical values used in Figure 4A are listed in Table S11; these demonstrate that the ensemble learning method outperforms the other three methods with respect to accuracy, precision, sensitivity and specificity. The ROC chart plotted in Figure 4B compares the classification effects of LR, Naive Bayes, SVM, and ensemble learning models. The classification effect of ensemble learning models is also superior to the other three.

Figure 4

4 Discussion

This study aimed to interrogate the potential therapeutic targets of SAH and use them as classifiers to develop a model for early prediction of SAH.

To achieve this aim, we proposed the following three scientific questions. First, is specific intervention involving LCN2 a promising SAH treatment strategy? Second, could we choose potential biomarkers for SAH at a genome-wide level by considering the effects of LCN2? Third, could we use key genes to build an SAH early prediction model with strong predictive power?

Regarding the first question, as the manually reviewed experimental evidence (Osuka et al., 2006;Majdalawieh et al., 2007;Hanafy et al., 2010;Hao et al., 2014;Kwon et al., 2015;Yu et al., 2018) and the results in Table 3 all indicate that LCN2-related signaling pathways play an important part in the pathogenesis SAH, we propose that LCN2 could promote or alleviate SAH-related diseases, and could also be used to treat SAH in the future.

To answer the second question, we used mathematical algorithms to explore five potential gene biomarkers (Tk1, Cyr61, Olig1, Slc6a9, and Pcolce2), considering the impact of both SAH and LCN2 treatment at different time points, and also used the manually reviewed experimental evidence to demonstrate that Cyr61 (Yu et al., 2018), Olig1 (Sabo et al., 2017), and Slc6a9 (Huang et al., 2016) were closely related to SAH. Although Tk1 and Pcolce2 have not been reported to be associated with SAH, we will investigate their connections in future work.

Regarding the third question, although this study represents significant progress in SAH prediction, it had several drawbacks. For example, the SAH intervention experiment sample size was too small for us to demonstrate high predictive accuracy for the model. In future work, we will integrate more recent bioinformatics research algorithms (Zhang et al., 2016;Gao et al., 2017;Zhang et al., 2017a;Zhang and Zhang, 2017;Zhang et al., 2018;Zhang et al., 2019a;Zhang et al., 2019d) and data into the system to overcome the problems.

In summary, this study analyzed the impact of LCN2 on SAH and explored the key biomarkers of SAH under LCN2 treatment at different time points. An ensemble learning model was developed to predict SAH occurrence. The results demonstrate that LCN2 (Warszawska et al., 2013) can effectively intervene in or treat SAH from a cell signaling pathway perspective. Also, three key genes were identified and validated by manual review of the experimental evidence (Huang et al., 2016;Sabo et al., 2017;Yu et al., 2018). Finally, the results showed that the ensemble learning model performed better for early SAH prediction than the classical LR, SVM, and naive-Bayes models.

5 Acknowledgments

This work has been supported in part by the National Science and Technology Major Innovation Program (No. 2018ZX10201002) and supported by the National Natural Science Foundation of China (NO.61372138) and the Southwest Hospital (SWH2018BJKJ-05).

6 Conflict of Interest

The authors declare that the research was conducted in the absence of any commercial or financial relationships that could be construed as a potential conflict of interest.

7 Author Contributions

LZ and YJC conceived the study and developed the model. HZ and WJL performed the simulations for the model. WJL and HZ wrote the manuscript. MX and HRZ performed the analysis for the model. HF, XFR and LQ contributed to acquisition of data. All authors read and approved the final manuscript.

8 Reference

Ai, C., Kong, L., and Genomics (2018). CGPS: A machine learning-based approach integrating multiple gene set analysis tools for better prioritization of biologically relevant pathways. *Journal of Genetics* 45**,** 489-504.

Armstrong, C.W., Bosio, E., Neil, C., Brown, S.G., Hankey, G.J., and Fatovich, D.M. (2017). Distinct inflammatory responses differentiate cerebral infarct from transient ischaemic attack. *Journal of Clinical Neuroscience* 35**,** 97-103.

Carlin, B.P., and Louis, T.A. (2010). *Bayes and empirical Bayes methods for data analysis*. Chapman and Hall/CRC.

Chaitanya, G., Schwaninger, M., Alexander, J., and Babu, P.P. (2010). Granzyme-b is involved in mediating post-ischemic neuronal death during focal cerebral ischemia in rat model. *Neuroscience* 165**,** 1203-1216.

Chu, S., Feng, D., Ma, Y., Zhang, H., Zhu, Z.A., Li, Z., and Zhang, Z. (2011). Expression of HGF and VEGF in the cerebral tissue of adult rats with chronic hydrocephalus after subarachnoid hemorrhage. *Molecular Medicine Reports* 4**,** 785-791.

Dietterich, T.G. (Year). "Ensemble methods in machine learning", in: *International workshop on multiple classifier systems*: Springer), 1-15.

Duan, K.-B., Rajapakse, J.C., Wang, H., and Azuaje, F. (2005). Multiple SVM-RFE for gene selection in cancer classification with expression data. *IEEE transactions on nanobioscience* 4**,** 228-234.

Edwards, J.W., Page, G.P., Gadbury, G., Heo, M., Kayo, T., Weindruch, R., and Allison, D.B. (2005). Empirical Bayes estimation of gene-specific effects in micro-array research. *Functional & integrative genomics* 5**,** 32-39.

Egashira, Y., Hua, Y., Keep, R.F., and Xi, G. (2014). Acute white matter injury after experimental subarachnoid hemorrhage: potential role of lipocalin 2. *Stroke* 45**,** 2141-2143.

Ferreira, A.C., Mesquita, S.D., Sousa, J.C., Correianeves, M., Sousa, N., Palha, J.A., and Marques, F. (2015). From the periphery to the brain: Lipocalin-2, a friend or foe? *Progress in Neurobiology* 131**,** 120-136.

Flo, T.H., Smith, K.D., Sato, S., Rodriguez, D., Holmes, M.A., Strong, R.K., Akira, S., and Aderem, A. (2004). Lipocalin 2 mediates an innate immune response to bacterial infection by sequestrating iron. *Nature* 432**,** 917-921.

Frontera, J.A., Claassen, J., Schmidt, J.M., Wartenberg, K.E., Temes, R., Connolly, E.S., Macdonald, R.L., and Mayer, S.A. (2006). Prediction of symptomatic vasospasm after subarachnoid hemorrhage: the modified fisher scale. *Neurosurgery* 59**,** 21-27.

Gao, H., Yin, Z., Cao, Z., and Zhang, L. (2017). Developing an Agent-Based Drug Model to Investigate the Synergistic Effects of Drug Combinations. *Molecules* 22**,** 2209.

Gautier, L., Cope, L., Bolstad, B.M., and Irizarry, R.A. (2004). affy—analysis of Affymetrix GeneChip data at the probe level. *Bioinformatics* 20**,** 307-315.

Guo, D., Wilkinson, D.A., Thompson, B.G., Pandey, A.S., Keep, R.F., Xi, G., and Hua, Y. (2017). MRI Characterization in the Acute Phase of Experimental Subarachnoid Hemorrhage. *Translational Stroke Research* 8**,** 234-243.

Hanafy, K.A., Grobelny, B., Fernandez, L., Kurtz, P., Connolly, E., Mayer, S.A., Schindler, C., and Badjatia, N. (2010). Brain interstitial fluid TNF-α after subarachnoid hemorrhage. *Journal of the neurological sciences* 291**,** 69-73.

Hao, X.-K., Wu, W., Wang, C.-X., Xie, G.-B., Li, T., Wu, H.-M., Huang, L.-T., Zhou, M.-L., Hang, C.-H., and Shi, J.-X. (2014). Ghrelin alleviates early brain injury after subarachnoid hemorrhage via the PI3K/Akt signaling pathway. *Brain research* 1587**,** 15-22.

Hosmer Jr, D.W., Lemeshow, S., and Sturdivant, R.X. (2013). *Applied logistic regression.* John Wiley & Sons.

Huang, B., Xie, Q., Lu, X., Qian, T., Li, S., Zhu, R., Yu, W., Chen, G., Chen, Z., and Xu, X. (2016). GlyT1 Inhibitor NFPS Exerts Neuroprotection via GlyR Alpha1 Subunit in the Rat Model of Transient Focal Cerebral Ischaemia and Reperfusion. *Cellular Physiology Biochemistry* 38**,** 1952-1962.

Irizarry, R.A., Hobbs, B., Collin, F., Beazer‐Barclay, Y.D., Antonellis, K.J., Scherf, U., and Speed, T.P. (2003). Exploration, normalization, and summaries of high density oligonucleotide array probe level data. *Biostatistics* 4**,** 249-264.

Kao, S.-C., Wu, H., Xie, J., Chang, C.-P., Ranish, J.A., Graef, I.A., and Crabtree, G.R. (2009). Calcineurin/NFAT signaling is required for neuregulin-regulated Schwann cell differentiation. *Science* 323**,** 651-654.

Kwon, M., Woo, S., Kurland, D., Yoon, S., Palmer, A., Banerjee, U., Iqbal, S., Ivanova, S., Gerzanich, V., and Simard, J. (2015). Methemoglobin is an endogenous Toll-like receptor 4 ligand—relevance to subarachnoid hemorrhage. *International journal of molecular sciences* 16**,** 5028-5046.

Lee, T.I., and Young, R.A. (2013). Transcriptional regulation and its misregulation in disease. *Cell* 152**,** 1237-1251.

Li, T., Cheng, Z., and Zhang, L. (2017). Developing a Novel Parameter Estimation Method for Agent-Based Model in Immune System Simulation under the Framework of History Matching: A Case Study on Influenza A Virus Infection. *Int J Mol Sci* 18.

Liu, G.-D., Li, Y.-C., Zhang, W., and Zhang, L. (2019). A Brief Review of Artificial Intelligence Applications and Algorithms for Psychiatric Disorders. *Engineering*.

Macdonald, R.L. (2014). Delayed neurological deterioration after subarachnoid haemorrhage. *Nature Reviews Neurology* 10**,** 44.

Macdonald, R.L., Kassell, N.F., Mayer, S., Ruefenacht, D., Schmiedek, P., Weidauer, S., Frey, A., Roux, S., and Pasqualin, A. (2008). Clazosentan to overcome neurological ischemia and infarction occurring after subarachnoid hemorrhage (CONSCIOUS-1) randomized, double-blind, placebo-controlled phase 2 dose-finding trial. *Stroke* 39**,** 3015-3021.

Majdalawieh, A., Zhang, L., and Ro, H.S. (2007). Adipocyte enhancer-binding protein-1 promotes macrophage inflammatory responsiveness by up-regulating NF-kappaB via IkappaBalpha negative regulation. *Mol Biol Cell* 18**,** 930-942.

Marta, R., and Marc, R.R. (2014). IQRray, a new method for Affymetrix microarray quality control, and the homologous organ conservation score, a new benchmark method for quality control metrics. *Bioinformatics***,** 10.

Ni, W., Gu, Y., Song, D.L., Leng, B., Li, P., and Mao, Y. (2011). The Relationship Between IL-6 in CSF and Occurrence of Vasospasm After Subarachnoid Hemorrhage. *Acta neurochirurgica* 110**,** 203-208.

Olabisi, O.A., Soto-Nieves, N., Nieves, E., Yang, T.T., Yang, X., Raymond, Y., Suk, H.Y., Macian, F., and Chow, C.-W. (2008). Regulation of transcription factor NFAT by ADP-ribosylation. *Molecular and cellular biology* 28**,** 2860-2871.

Osuka, K., Watanabe, Y., Yamauchi, K., Nakazawa, A., Usuda, N., Tokuda, M., and Yoshida, J. (2006). Activation of the JAK-STAT signaling pathway in the rat basilar artery after subarachnoid hemorrhage. *Brain research* 1072**,** 1-7.

Ramos, L.A., Van Der Steen, W.E., Barros, R.S., Majoie, C.B., Van Den Berg, R., Verbaan, D., Vandertop, W.P., Zijlstra, I.J.a.J., Zwinderman, A., and Strijkers, G.J. (2019). Machine learning improves prediction of delayed cerebral ischemia in patients with subarachnoid hemorrhage. *Journal of neurointerventional surgery* 11**,** 497-502.

Roederer, A., Holmes, J.H., Smith, M.J., Lee, I., and Park, S. (2014). Prediction of significant vasospasm in aneurysmal subarachnoid hemorrhage using automated data. *Neurocritical care* 21**,** 444-450.

Sabo, J.K., Heine, V., Silbereis, J.C., Schirmer, L., Levison, S.W., and Rowitch, D.H. (2017). Olig1 is required for noggin‐induced neonatal myelin repair. *Annals of neurology* 81**,** 560-571.

Smyth, G.K. (2005). "Limma: linear models for microarray data," in *Bioinformatics and computational biology solutions using R and Bioconductor*. Springer), 397-420.

Sozen, T., Tsuchiyama, R., Hasegawa, Y., Suzuki, H., Jadhav, V., Nishizawa, S., and Zhang, J.H. (2011). Immunological Response in Early Brain Injury After SAH. *Acta neurochirurgica* 110**,** 57-61.

Suarez, J.I., Tarr, R.W., and Selman, W.R. (2006). Aneurysmal subarachnoid hemorrhage. *New England Journal of Medicine* 354**,** 387-396.

Suykens, J.A., and Vandewalle, J. (1999). Least squares support vector machine classifiers. *Neural processing letters* 9**,** 293-300.

Varet, H., Brillet-Guéguen, L., Coppée, J.-Y., and Dillies, M.-A. (2016). SARTools: a DESeq2-and edgeR-based R pipeline for comprehensive differential analysis of RNA-Seq data. *PloS one* 11**,** e0157022.

Wang, Q., Garrity, G.M., Tiedje, J.M., and Cole, J.R. (2007). Naive Bayesian classifier for rapid assignment of rRNA sequences into the new bacterial taxonomy. *Appl. Environ. Microbiol.* 73**,** 5261-5267.

Warszawska, J., Gawish, R., Sharif, O., Sigel, S., Doninger, B., Lakovits, K., Mesteri, I., Nairz, M., Boon, L., and Spiel, A.O. (2013). Lipocalin 2 deactivates macrophages and worsens pneumococcal pneumonia outcomes. *Journal of Clinical Investigation* 123**,** 3363-3372.

Wu, J., Mao, X., Cai, T., Luo, J., and Wei, L. (2006). KOBAS server: a web-based platform for automated annotation and pathway identification. *Nucleic Acids Research* 34**,** 720-724.

Wu, W., and Zhang, L. (2020). Exploring the dynamics and interplay of human papillomavirus and cervical tumorigenesis by integrating biological data into a mathematical model. *BMC Bioinformatics*.

Xia, Y., Yang, C., Hu, N., Yang, Z., He, X., Li, T., and Zhang, L. (2017). Exploring the key genes and signaling transduction pathways related to the survival time of glioblastoma multiforme patients by a novel survival analysis model. *BMC genomics* 18**,** 950.

Xiao, M., Yang, X., Yu, J., and Zhang, L. (2019a). CGIDLA: Developing the Web Server for CpG Island related Density and LAUPs (Lineage-associated Underrepresented Permutations) Study. *IEEE/ACM Trans Comput Biol Bioinform*.

Xiao, M., Yang, X., Yu, J., and Zhang, L. (2019b). CGIDLA: Developing the Web Server for CpG Island related Density and LAUPs (Lineage-associated Underrepresented Permutations) Study. *IEEE/ACM transactions on computational biology and bioinformatics*.

Xie, C., Mao, X., Huang, J., Ding, Y., Wu, J., Dong, S., Kong, L., Gao, G., Li, C.-Y., and Wei, L. (2011). KOBAS 2.0: a web server for annotation and identification of enriched pathways and diseases. *Nucleic acids research* 39**,** W316-W322.

Yu, S., Zeng, Y.J., and Sun, X.C. (2018). Neuroprotective effects of p53/microRNA-22 regulate inflammation and apoptosis in subarachnoid hemorrhage. *International Journal of Molecular Medicine* 41**,** 2406-2412.

Zhang, L., Bai, W., Yuan, N., and Du, Z. (2019a). Comprehensively benchmarking applications for detecting copy number variation. *PLoS Comput Biol* 15**,** e1007069.

Zhang, L., Li, J., Yin, K., Jiang, Z., Li, T., Hu, R., Yu, Z., Feng, H., and Chen, Y. (2019b). Computed tomography angiography-based analysis of high-risk intracerebral haemorrhage patients by employing a mathematical model. *BMC Bioinformatics* 20**,** 193.

Zhang, L., Li, P., Zhao, J., Yang, X., Li, Z., and Yu, J. (2019c). Research progress on the three-dimensional structure of genome. *SCIENTIA SINICA Vitae*.

Zhang, L., Liu, Y., Wang, M., Wu, Z., Li, N., Zhang, J., and Yang, C.B. (2017a). EZH2-, CHD4-, and IDH-linked epigenetic perturbation and its association with survival in glioma patients. *Journal of Molecular Cell* 9**,** 477-488.

Zhang, L., Liu，G., Kong, M., Li, T., Wu, D., Zhou, X., Yang, C., Xia, L., Yang, Z., and Chen，Ln. (2019d). Revealing dynamic regulations and the related key proteins of myeloma-initiating cells by integrating experimental data into a systems biological model. *Bioinformatics*.

Zhang, L., Qiao, M., Gao, H., Hu, B., Tan, H., Zhou, X., and Li, C.M. (2016). Investigation of mechanism of bone regeneration in a porous biodegradable calcium phosphate (CaP) scaffold by a combination of a multi-scale agent-based model and experimental optimization/validation. *Nanoscale* 8**,** 14877-14887.

Zhang, L., Xiao, M., Zhou, J., and Yu, J. (2018). Lineage-associated underrepresented permutations (LAUPs) of mammalian genomic sequences based on a Jellyfish-based LAUPs analysis application (JBLA). *Bioinformatics* 34**,** 3624-3630.

Zhang, L., and Zhang, S. (2017). Using game theory to investigate the epigenetic control mechanisms of embryo development: Comment on: "Epigenetic game theory: How to compute the epigenetic control of maternal-to-zygotic transition" by Qian Wang et al. *Phys Life Rev* 20**,** 140-142.

Zhang, L., Zheng, C.Q., Li, T., Xing, L., Zeng, H., Li, T.T., Yang, H., Cao, J., Chen, B.D., and Zhou, Z.Y. (2017b). Building Up a Robust Risk Mathematical Platform to Predict Colorectal Cancer. *Complexity* 2017**,** 14.

Zhang, L., Zichun, D., Jun, Y., and Ming, X. (2020). CpG-island-based annotation and analysis of human housekeeping genes. *Briefings in Bioinformatics*.

Zou, H., Hastie, T., and Tibshirani, R. (2006). Sparse principal component analysis. *Journal of computational and graphical statistics* 15**,** 265-286.

TABLE AND FIGURES LEGENDS

Figure 1. Workflow of the study. (A) SAH intervention experimental chip RLE box line diagram; the abscissa is log_2 (Median value of sample expression) and the ordinate represents each chip; (B) The volcano map of the comparison group SAH-siRNA-NC (1 day) vs normal-2. The abscissa is $log_2(Fold\ change)$ and the ordinate is $-log_{10}(FDR)$; The red point is the up-regulated gene, the blue point is the down-regulated gene, and the non-dispersive point is the non-differentiated gene; (C) Key gene screening workflow; (D) The accuracy for ensemble learning, LR, SVM and Naive-Bayes.

Figure 2. Venn plot for the key genes

Figure 3. SAH predictive ensemble learning model

Figure 4. Model performance. (A) Comparison of classification performance of LR, SVM , Naive-Bayes and ensemble learning model; (B) ROC chart plotted for LR, SVM , Naive-Bayes and ensemble learning model.

478 **Table 1. Experimental sample description after LCN2 intervention experiment.**

Sample	Number of samples	Description
SAH-siRNA-LCN2(1day)	5	Mouse (SAH) brain cells, Intrathecal injection of LCN2 siRNA for 1 day
SAH-siRNA-LCN2(3day)	5	Mouse (SAH) brain cells, Intrathecal injection of LCN2 siRNA for 3 day
SAH-siRNA-NC(1day)	5	Mouse (SAH) brain cells, Intrathecal injection of blank siRNA for 1 day
SAH-siRNA-NC(3day)	5	Mouse (SAH) brain cells, Intrathecal injection of blank siRNA for 3 day
normal-2	5	Mouse (normal) brain cells, blank control group-2

479

480

481 **Table 2. Differential expressed genes for different experimental group.**

Experimental group	Total number of genes	Up-regulation of genes	Down-regulation of genes
SAH-siRNA-LCN2(1day) VS normal-2	25342	1541	634
SAH-siRNA-LCN2 (3day) VS normal-2	25055	1264	451
SAH-siRNA-NC(1day) VS normal-2	25384	1159	556
SAH-siRNA-NC(3day) VS normal-2	25564	1297	409
SAH-siRNA- LCN2 (1day) VS SAH-siRNA-NC(1day)	25293	99	14
SAH-siRNA- LCN2 (3day) VS SAH-siRNA-NC(3day)	25251	5	18

482

483

484 **Table 3. Cross-validated SAH related signaling pathway.**

Experimental group	Important pathways related to SAH
SAH-siRNA-LCN2(1day) VS normal-2	PI3K-Akt(Hao et al., 2014), Jak-STAT(Osuka et al., 2006), p53(Yu et al., 2018), TNF(Hanafy et al., 2010), Toll-like receptor(Kwon et al., 2015), NF-kappaβ(Majdalawieh et al., 2007)
SAH-siRNA-LCN2 (3day) VS normal-2	PI3K-Akt(Hao et al., 2014), Jak-STAT(Osuka et al., 2006), p53(Yu et al., 2018), TNF(Hanafy et al., 2010), Toll-like receptor(Kwon et al., 2015), NF-kappaβ(Majdalawieh et al., 2007)
SAH-siRNA-NC(1day) VS normal-2	PI3K-Akt(Hao et al., 2014), Jak-STAT(Osuka et al., 2006), TNF(Hanafy et al., 2010), Toll-like receptor(Kwon et al., 2015), NF-kappaβ(Majdalawieh et al., 2007)
SAH-siRNA-NC(3day) VS normal-2	PI3K-Akt(Hao et al., 2014), Jak-STAT(Osuka et al., 2006), TNF(Hanafy et al., 2010), Toll-like receptor(Kwon et al., 2015), NF-kappaβ(Majdalawieh et al., 2007)
SAH-siRNA- LCN2 (1day) VS SAH-siRNA-NC(1day)	TNF(Hanafy et al., 2010), Toll-like receptor(Kwon et al., 2015)
SAH-siRNA- LCN2 (3day) VS SAH-siRNA-NC(3day)	Transcriptional misregulation in cancer(Lee and Young, 2013)

485

Supplementary Material

1 Supplementary Figures and Tables

1.1 Supplementary Figures

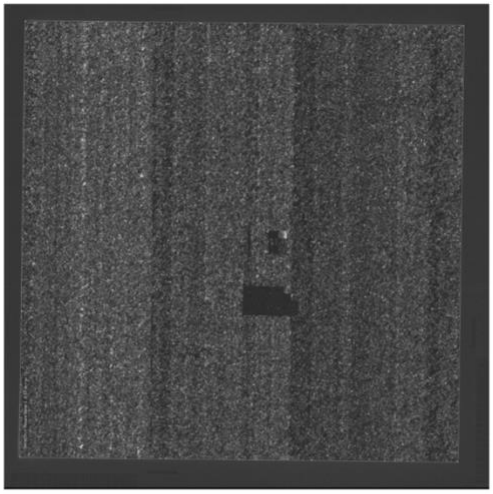

(A) SAH_1

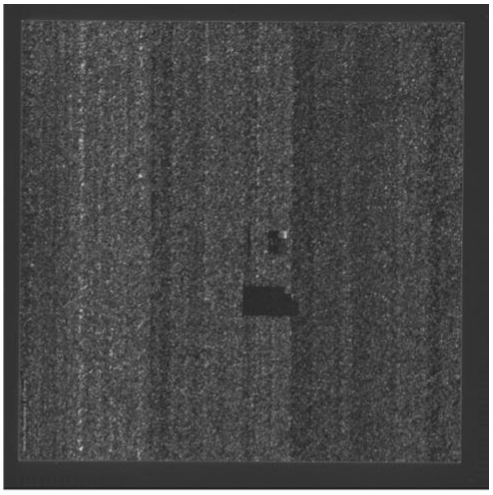

(B) SAH_2

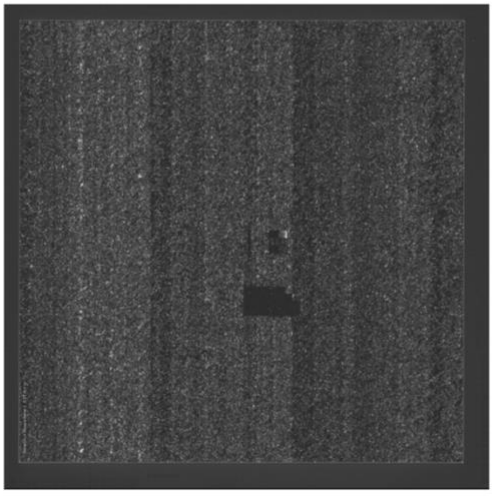

(C) SAH_3

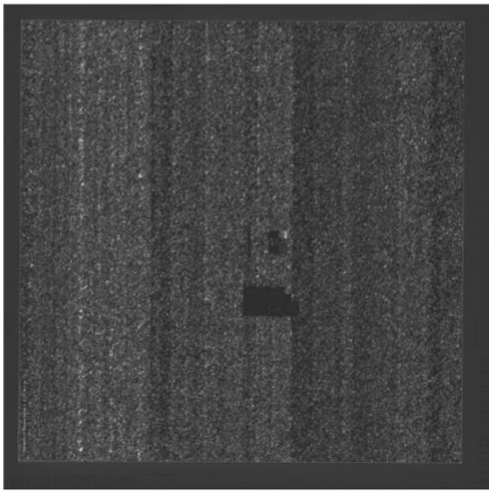

(**D**) SAH_4

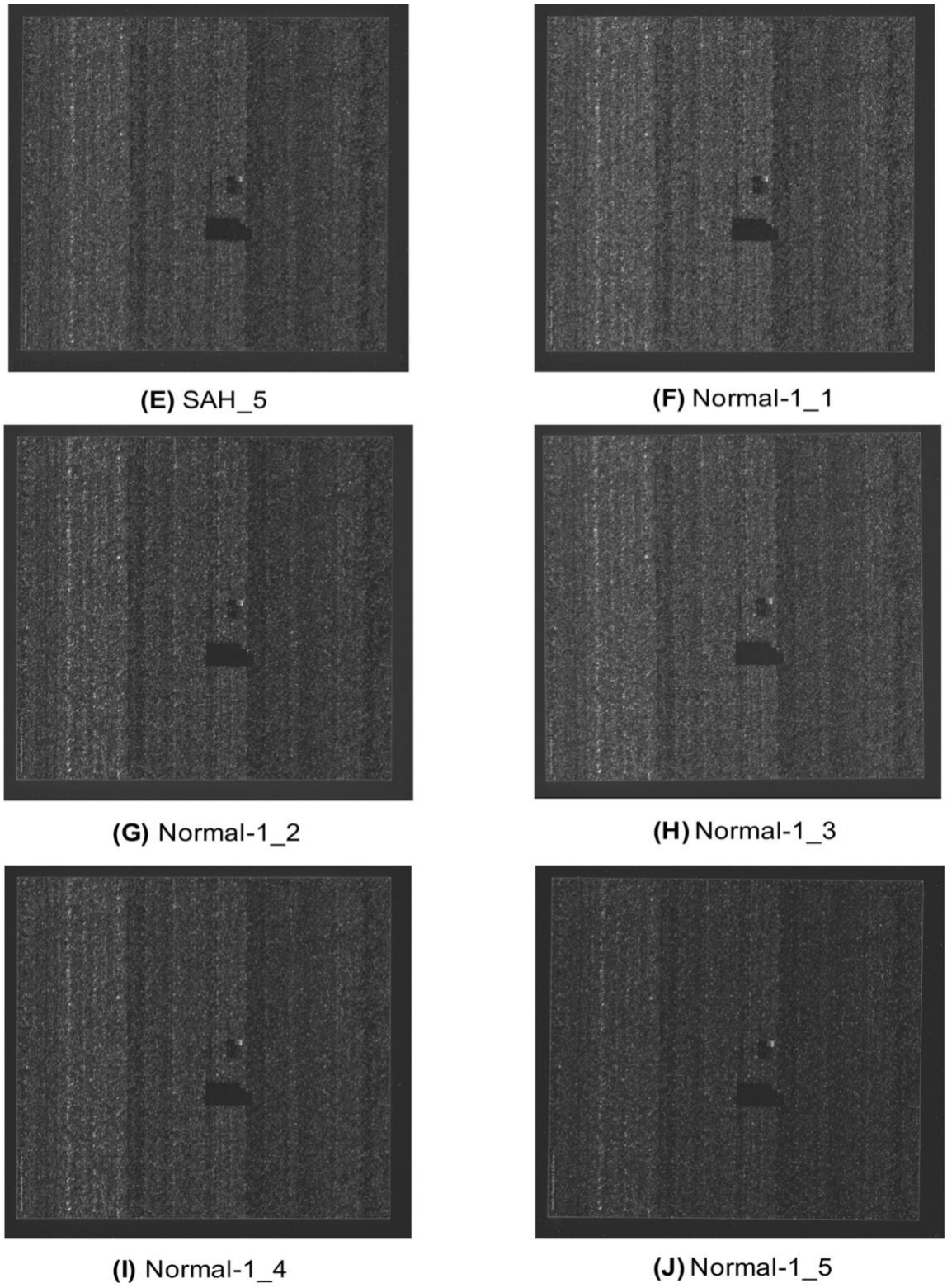

Figure S1. Gray scale image for SAH intervention experiment. Ten original chip gray scale images of SAH intervention experiment; **(A)-(E)** are the gray scale images for five experimental group chips; **(F)-(J)** are the gray scale images for five control group chips.

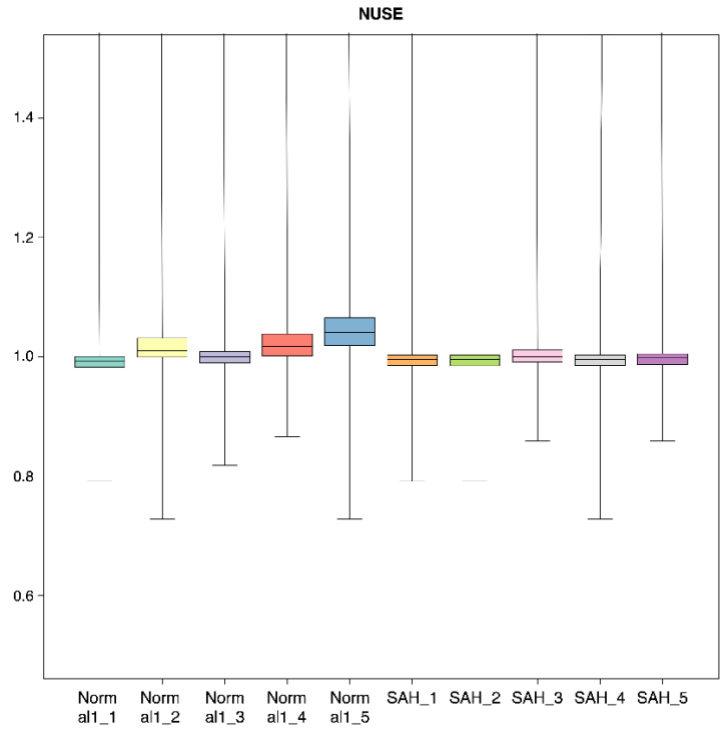

Figure S2. SAH intervention experimental chip NUSE boxplot.

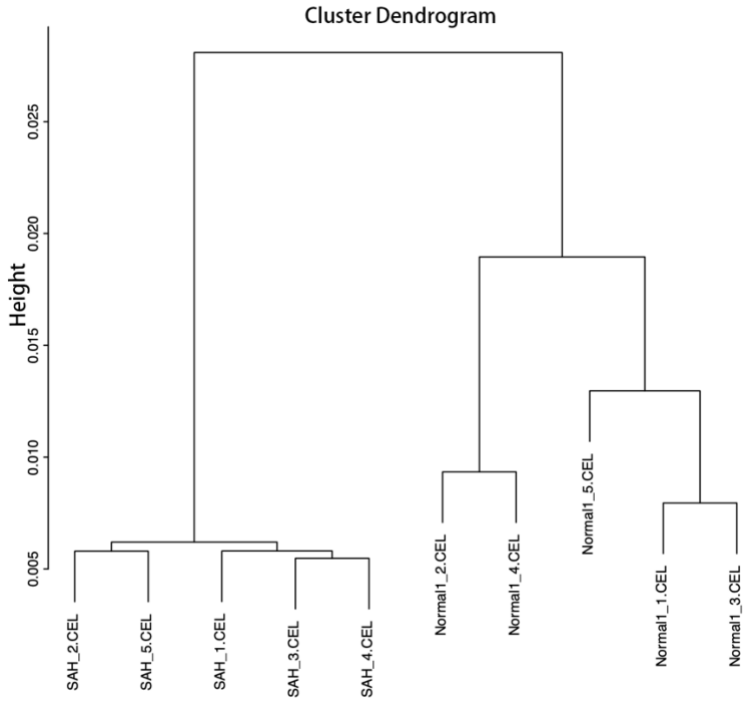

Figure S3. Cluster graph for SAH intervention experiment.

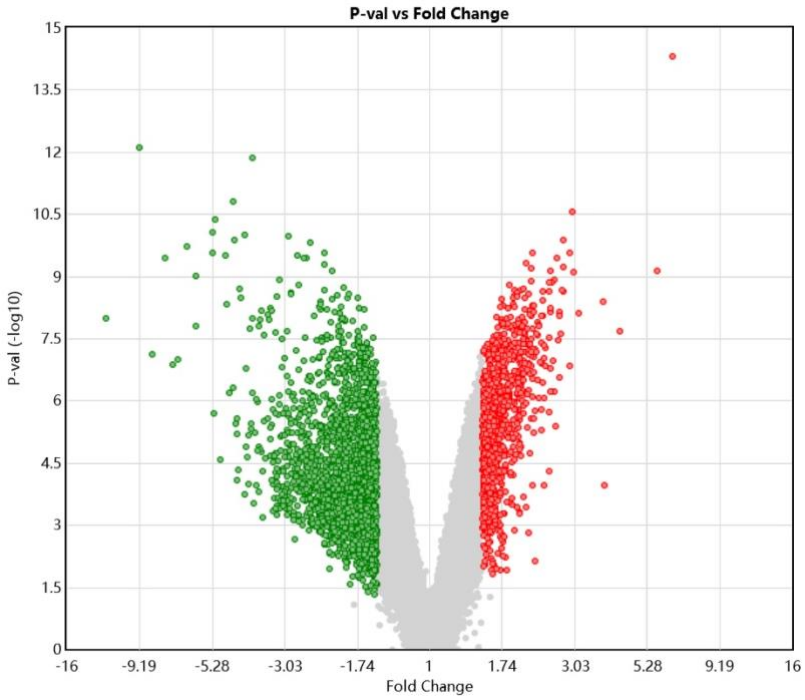

Figure S4. Volcanic maps for SAH intervention experiment. The volcano map of the comparison group SAH vs normal-1. The abscissa is $log_2(Fold\ change)$ and the ordinate is $-log_{10}(FDR)$. The red, green and non-dispersive points represent the up-regulated, down-regulated, and non-differentiated gene, respectively.

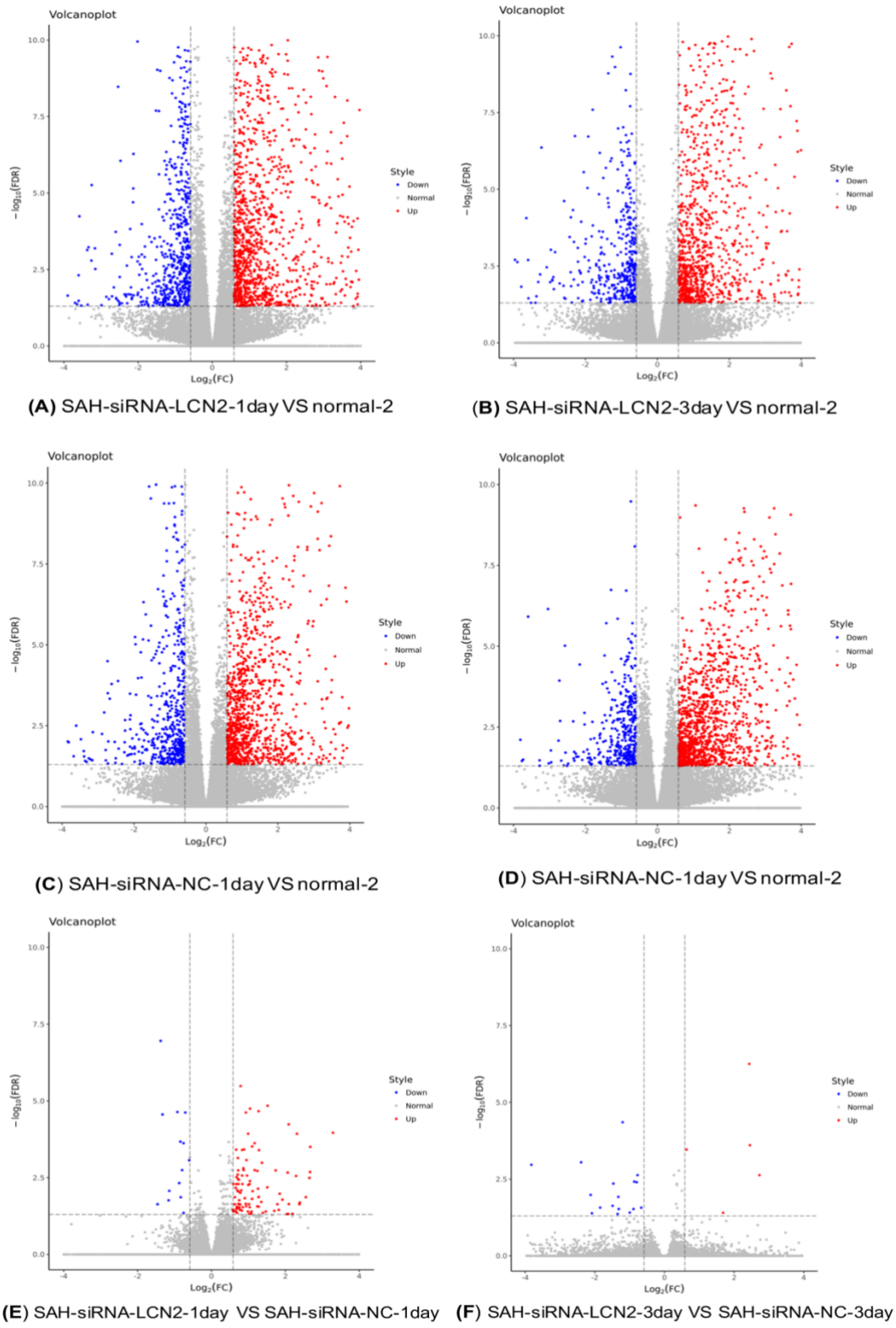

Figure S5. Volcanic maps for LCN2 intervention experiment. The volcano map of the different group. The abscissa is $log_2(Fold\ change)$ and the ordinate is $-log_{10}(FDR)$. The red, blue and non-dispersive points represent the up-regulated, down-regulated, and non-differentiated gene, respectively.

1.2 Supplementary Tables

Table S1. Probes expression data matrix.

The experimental probe expression matrix for each group in the SAH intervention experiment.

Table S2. SAH intervention experiment analysis results.

The results of differentially expressed gene analysis and related signaling pathway analysis in SAH intervention experiments.

Table S3. Fisher's exact Test for the signaling pathway.

	Differentially expressed gene	Non-differentiated gene	Total
Included in pathway	n_f	$n - n_f$	n
Not included in pathway	$N_f - n_f$	$(N - n_f) - (n - n_f)$	$N - n$
Total	N_f	$N - N_f$	N

Table S4. Differential genetic analysis results for LCN2 interventional experiments.

Results of differential genetic analysis for each group of data in the LCN2 intervention experiment.

Table S5. Signaling pathway analysis results for LCN2 intervention experiments.

Results of signaling pathway analysis of each group of data in the LCN2 intervention experiment.

TableS1, S2, S4 and S5 are available on https://github.com/charlotte5683/supplementary-of-SAH.git.

Table S6. 47 key genes for both e-Bayes and SVM-RFE methods.

Gene name

Cyb5r1	Pcolce2
Kcnt2	Tagln
Ddr2	mt-Tr
Igf1	mt-Ts2
Lum	Slc7a3
Dusp6	Capn6
Tk1	Tnfsf18
Gm24564	Gm39701
Pck2	Moxd1
Tmem74	Dcn
Zfp942	Aldh1l2
Ttr	Meg3
Stk32a	Ero1l
Chac1	Enpp2
Trib3	Mir99ahg
Postn	Olig1
Slc7a11	Ankrd12
Cyr61	Acta2
Slc6a9	Fbln7
Akap9	P2rx3
Mir344-2	Cth

Trim66	Gabra2
Nupr1	Cyb5r2
Ednra	

Table S7. Significantly differential genes for SAH-siRNA-LCN2(1day) VS normal-2 group.

SAH-siRNA-LCN2(1day) VS normal-2 group	
Olig1	Pck2
Cyb5r1	Kcnt2
Tk1	Nupr1
Dcn	Lum
Ednra	Pcolce2
Slc6a9	Slc7a11
Cyr61	Trib3
Akap9	

Table S8. Significantly differential genes for SAH-siRNA-LCN2(3day) VS normal-2 group.

SAH-siRNA-LCN2(3day) VS normal-2 group	
Tk1	Slc6a9
Cyr61	Dusp6
Aldh1l2	Olig1

Nupr1	Igf1
Dcn	Kcnt2
Lum	
Pcolce2	
Tnfsf18	

Table S9. Input samples for the prediction model.

Gene Name	SAH_1	SAH_2	SAH_3	SAH_4	SAH_5
Cyr61	5.8942628	5.96110867	5.93479255	6.02621404	5.73609078
Olig1	7.0429023	7.56910104	7.21385307	7.27041593	7.43777252
Slc6a9	9.4912445	9.20928367	9.54588542	9.43792448	9.01581096
Gene Name	**Normal-1_1**	**Normal-1_2**	**Normal-1_3**	**Normal-1_4**	**Normal-1_5**
Cyr61	7.3059794	7.56463002	7.19854145	7.74025933	7.38489239
Olig1	8.8771356	9.18547761	8.8943184	9.011647	8.88975631
Slc6a9	7.1622279	7.28458596	7.34258084	7.42990633	7.09533177

Table S10. Model performance indicator.

Index	Formula	Illustration
Accuracy	$\frac{TP+TN}{P+N}$	TP: actual illness and is recognized as disease
Precision	$\frac{TP}{TP+FP}$	TN: not actually diseased and is recognized as a disease

Sensitivity	$\frac{TP}{TP+FN}$	FP： not actually affected, but it is recognized as a disease
Specificity	$\frac{TN}{FP+TN}$	FN: actual illness, but was identified as being unaffected

Table S11. Model performance statistic.

	LR	SVM	Naive-Bayes	Ensemble
Accuracy	0.612500±0.074789	0.518750±0.035013	0.497917±0.058101	0.789583±0.108943
Precision	0.660069±0.155874	0.527778±0.139916	0.565625±0.135964	0.765104±0.141375
Sensitivity	0.631944±0.160185	0.621528±0.167532	0.729167±0.127047	0.87500±0.105263
Specificity	0.656250±0.227961	0.510417±0.252522	0.500000±0.252632	0.770833±0.178509

2 Supplementary Note

2.1 SAH intervention experiment

The mouse endovascular perforation model of SAH was induced as reported previously(Yujie et al., 2015;Amp and Wilkins, 2017). Briefly, mice were anesthetized with isoflurane. A sharpened 5-0 monofilament nylon suture was inserted rostrally into the left internal carotid artery from the external carotid artery stump and perforated the bifurcation of the anterior and middle cerebral arteries. Sham-operated mice underwent the same procedure without puncturing the artery. Tissues of white matters were taken for follow-up detection on day 3 after SAH.

The processed datasets for this study can be found in the github:

https://github.com/charlotte5683/SAH.git

ArrayExpress accession: E-MTAB-8407

https://www.ebi.ac.uk/arrayexpress/experiments/E-MTAB-8407/

2.2 LCN2 intervention experiment

According to methods described previously (Zuo et al., 2017), an intracerebroventricular injection was performed. Put simply, mice were placed on a stereotaxic apparatus (Rwdmall, Guangzhou, China) after anesthetized with 2% pentobarbital sodium (50 mg/kg, intraperitoneal). The bregma point was

then exposed and a small bone window was drilled into the bone of the left hemisphere. Then, 2 μL specific siRNAs was delivered into the lateral ventricle with a Hamilton syringe (Hamilton Company, Reno, NV, USA). The injection was performed 48 h before SAH. Tissues of white matters were taken for follow-up detection on day 1 and day 3 after SAH respectively.

The processed datasets for this study can be found in the github:

https://github.com/charlotte5683/LCN2.git

NCBI SRA accession: PRJNA575372

https://www.ncbi.nlm.nih.gov/sra/PRJNA575372

2.3 Code availability

Code used for predictive model is available at https://github.com/charlotte5683/SAH-code .

3 Reference

Amp, L.W., and Wilkins (2017). Correction to: Role of Periostin in Early Brain Injury After Subarachnoid Hemorrhage in Mice. *Stroke* 48**,** 1108-1111.

Yujie, C., Yang, Z., Junjia, T., Fei, L., Qin, H., Chunxia, L., Jiping, T., Hua, F., and Zhang, J.H. (2015). Norrin protected blood-brain barrier via frizzled-4/β-catenin pathway after subarachnoid hemorrhage in rats. *Stroke* 46**,** e91.

Zuo, S., Ge, H., Li, Q., Zhang, X., Hu, R., Hu, S., Liu, X., Zhang, J.H., Chen, Y., and Feng, H. (2017). Artesunate Protected Blood–Brain Barrier via Sphingosine 1 Phosphate Receptor 1/Phosphatidylinositol 3 Kinase Pathway After Subarachnoid Hemorrhage in Rats. *Molecular Neurobiology* 54**,** 1213-1228.